Journal of Instrumentation

Temperature dependence calibration and correction of the DAMPE BGO electromagnetic calorimeter

To cite this article: Y.F. Wei *et al* 2016 *JINST* **11** T07003

Published by IOP Publishing for Sissa Medialab

Received: *March 21, 2016*
Revised: *May 25, 2016*
Accepted: *June 23, 2016*
Published: *July 5, 2016*

TECHNICAL REPORT

2016 JINST 11 T07003

Temperature dependence calibration and correction of the DAMPE BGO electromagnetic calorimeter

Y.F. Wei,[a,b] **Z.Y. Zhang,**[a,b] **Y.L. Zhang,**[a,b,1] **S.C. Wen,**[a,b,c] **C. Wang,**[a,b] **Z.Y. Li,**[a,b] **C.Q. Feng,**[a,b] **X.L. Wang,**[a,b] **Z.Z. Xu,**[a,b] **G.S. Huang**[a,b] **and S.B. Liu**[a,b]

[a] *State Key Laboratory of Particle Detection and Electronics, University of Science and Technology of China, Hefei, Anhui 230026, China*

[b] *Department of Modern Physics, University of Science and Technology of China, Hefei, Anhui 230026, China*

[c] *Purple Mountain Observatory, Chinese Academy of Sciences, Nanjing, Jiangsu 210008, China*

E-mail: ylzhang@ustc.edu.cn

Abstract: A BGO electromagnetic calorimeter (ECAL) is built for the DArk Matter Particle Explorer (DAMPE) mission. The temperature effect on the BGO ECAL was investigated with a thermal vacuum experiment. The light output of a BGO crystal depends on temperature significantly, and the readout system is also affected by temperature. The temperature coefficient of each BGO detection unit has been calibrated, and a correction method is also presented in this paper.

Keywords: Calorimeters; Dark Matter detectors (WIMPs, axions, etc.)

ArXiv ePrint: 1604.08060

[1] Corresponding author.

doi:10.1088/1748-0221/11/07/T07003

Contents

2016 JINST 11 T07003

1 Introduction

The DArk Matter Particle Explorer project is a Chinese space detection mission seeking precise measurement of high-energy electrons, gamma rays and nuclei from deep space. It was launched at the end of 2015. So far, the physical origin of unexpected galactic electron/positron excesses [1–3] has yet to be figured out. DAMPE will provide a high energy resolution measurement of the (e^++e^-) spectrum from 5 GeV to 10 TeV, which has not been revealed by existing experiments in 1 TeV to 10 TeV ranges. DAMPE can also measure protons, helium nuclei, and other cosmic ions in the energy band from 10 GeV to 1 PeV [4].

The DAMPE detector consists of four sub-detectors (figure 1). The plastic scintillator detector (PSD) is used to identify electrons, photons and cosmic ions. The silicon tungsten tracker (STK) provides tracking. The neutron detector (NUD) is designed to improve the electron/proton separating capability for proton background rejection in space. The emphasis of this paper is the BGO electromagnetic calorimeter (BGO ECAL), which provides a high-precision measurement of energy.

The DAMPE satellite orbits the earth at an altitude of 500 km, and the designed maximum temperature variation of the BGO ECAL ranges from -15 °C to +20 °C under the satellite thermal control system. The ECAL is made up of 308 BGO crystal bars, each with dimensions of 25 × 25 × 600 mm^3. BGO is an inorganic crystal, and its scintillation light yield is strongly temperature dependent. A decrease of temperature leads to an increase of luminescence intensity. This property was studied since many years [5, 6]. The reference value of temperature dependence of a BGO crystal is -0.9% /°C (at room temperature) [7]. The Bialkali PMTs (Hamamatsu R5610A-01) used in the ECAL are also affected by temperature (anode sensitivity ~ -0.4% /°C) [8]. We investigated the temperature dependence with a BGO detection unit of the DAMPE quarter prototype [9]. In order to better understand the temperature performance of the full calorimeter, a thermal vacuum experiment of the DAMPE flight model was performed in July of 2015.

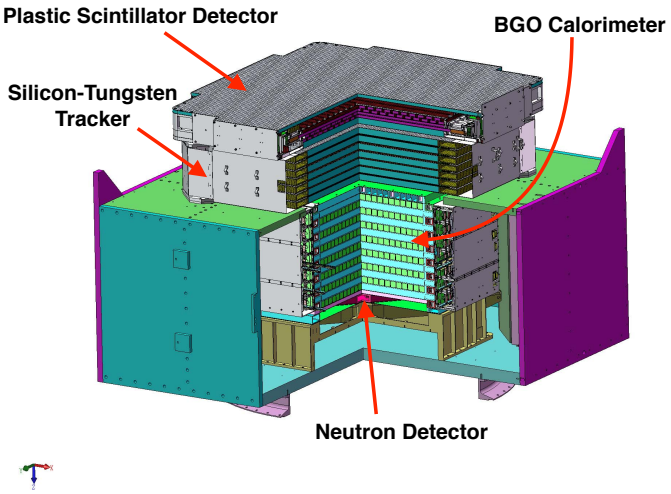

Figure 1. Structure of the DAMPE detector.

2 Design of the BGO ECAL

The BGO ECAL measures the energy deposition of particles with a wide range, from 5 GeV to 10 TeV, and with a good energy resolution of 1.5% at 800 GeV for photons and electrons. The ECAL contains 14 layers (31 radiation lengths), with 22 BGO crystal bars in each layer. The layers of BGO crystal bars are alternated in an orthogonal way to measure the deposited energy and profile of the hadron and electromagnetic showers developed in the BGO ECAL (figure 2). Scintillation light is detected at both sides of a BGO crystal bar with two PMTs. A single crystal and its readout system of one side constitute a detection unit. Figure 3 shows two detection units of one BGO crystal bar. The required range of energy response for one detection unit is from 10 MeV to 2 TeV. In order to obtain such a wide dynamic range, a multi-dynode readout circuit of the PMT base is used, and the dynode 2, 5 and 8 of a PMT correspond to low, middle, and high gain, respectively [10, 11]. Meanwhile, an asymmetrical design is applied in the readout of two side PMTs. The attenuation filter is designed to tune the amplitudes of signals by attenuating the flux of scintillation lights injecting into the PMT with optional factors [12]. One side signals (called Side 1, the other side is Side 0) in shower extension layers (layer 2 ~ layer 13) are more attenuated to contain a higher energy shower.

3 Thermal vacuum experiment

The primary goal of the thermal vacuum (TV) environmental experiment was to validate the thermal performance of the DAMPE flight model. For the BGO sub-detector, the cosmic ray data from the period of the TV experiment was utilized to study the temperature dependence. The DAMPE detector was held in a cylindrical chamber, and covered by a heating cage (figure 4). A liquid nitrogen cooling layer surrounded the instrument inside the chamber. There was also a thermally insulating layer between the DAMPE detector and the support platform.

Figure 5 shows the temperature variation measured by a thermistor attached on the surface of a BGO crystal bar. The precision of this kind of thermistor is 0.1 °C. There were one long cycle

2016 JINST 11 T07003

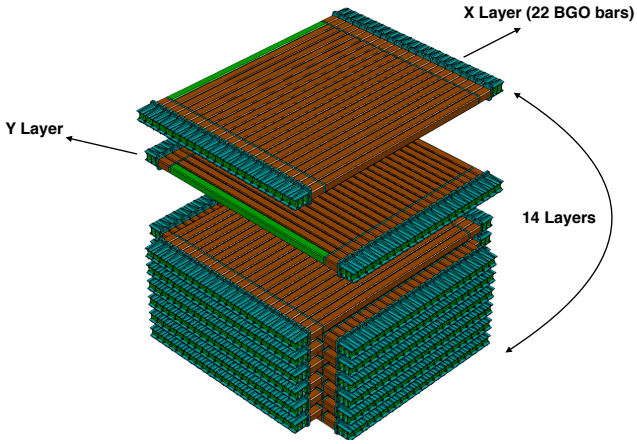

Figure 2. BGO crystal bars arrangement in the ECAL.

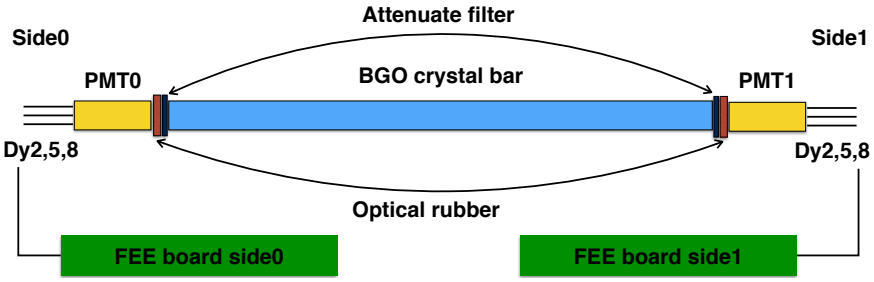

Figure 3. The detection unit of the BGO ECAL.

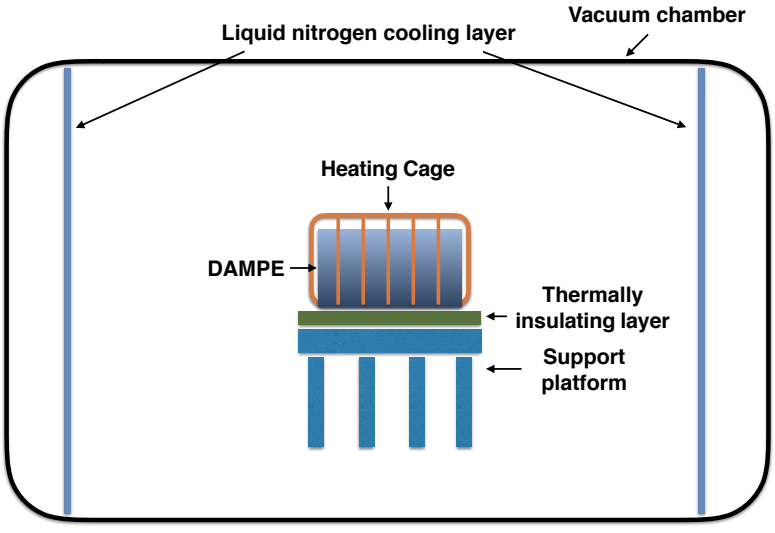

Figure 4. Thermal vacuum experiment setup.

2016 JINST 11 T07003

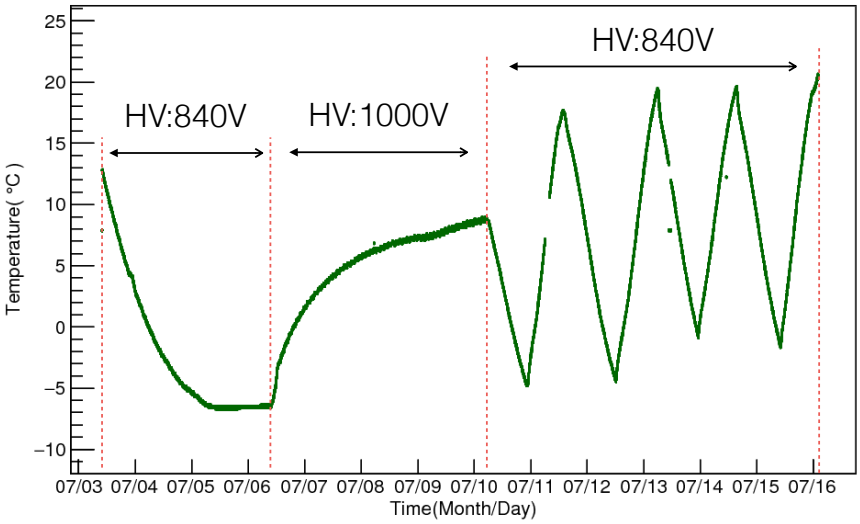

Figure 5. Temperature curve of one BGO crystal bar.

(July 2 ~ July 10) and four short cycles (July 10 ~ July 16) during the TV experiment. The change rate of temperature in the long cycle, which was no more than 1 °C/hour, was much gentler than the rate of change in the short cycle, therefore, temperature dependence was calibrated with the data from the long cycle. Since two high voltage working modes (800 V and 1000 V) are applied on orbit (800 V is normal mode), the experiment was conducted in these two modes, respectively. The periods of different high voltage modes are marked in figure 5.

4 Temperature dependence calibration

The contributions to the temperature effect of a detection unit are mainly from three parts: the BGO crystals, the PMTs and the electronics, however, it is difficult to measure the temperature dependence separately for these three parts after assembly of the BGO ECAL. Thus, we utilize the variation of calibration parameters to investigate the temperature performance of the BGO ECAL.

4.1 Temperature performances of the electronics

The BGO calorimeter has four vertical side (called quadrant), each with 154 PMTs and 462 (154×3) signal channels. On each quadrant, there are four FEEs (Front-End Electronics) taking charge of the readout task for detector signals. VA160 and VATA160 ASICs (Application Special Integrated Circuits) are the key components on the FEEs. They are responsible for integrating and shaping the PMT signals, with shaping time of about 1.8μs, and then sending out the amplitudes channel by channel [13]. Since the temperature variation may interfere the VA160s, the temperature performance of gain coefficient of chips was investigated in [14]. In a range of -15 °C to +25 °C, the gain decreased from 1.192 to 1.129, which was no more than -0.2% /°C.

2016 JINST 11 T07003

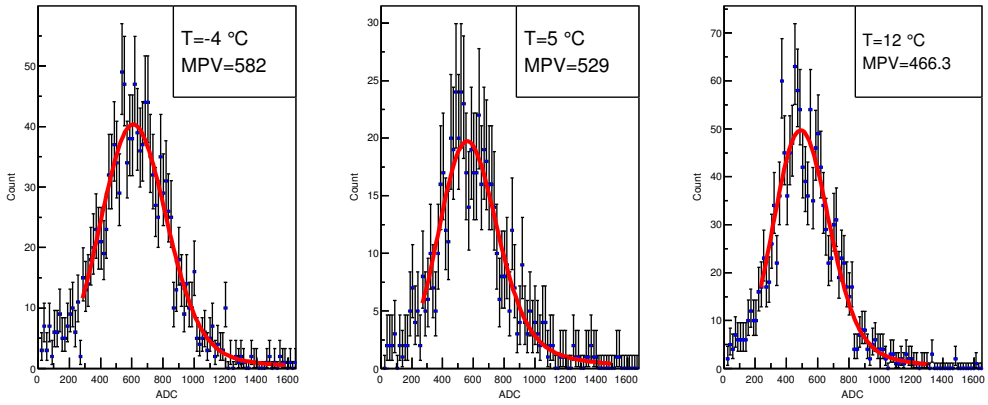

Figure 6. Cosmic ray muon spectra at different temperatures.

4.2 Temperature dependence of the detection units

On the ground level, the measurement of the muon minimum ionizing particle (MIP) energy could provide the absolute energy calibration for the BGO ECAL. The variation of the MIPs MPV (most probable value) indicates the temperature performance of the detection unit. We used the data from the long cycle in the TV test for temperature dependence calibration. Figure 6 shows the energy deposition spectra of muon MIPs at different temperatures. These spectra were fitted with Landau convoluted with Gaussian, and the Landau MPV values were used to represent the light output of BGO crystal bars. For an individual detection unit, the MPV value decreases with the increase of temperature (figure 7), and the variation trend may be well described by a linear function in this temperature range. The temperature coefficient is defined as equation (4.1):

$$C_t = \frac{\text{Slope of fit line}}{\text{Intercept of fit line}} \tag{4.1}$$

This coefficient is exactly the temperature dependence at 0 °C. Figure 8 shows the distribution of C_t values from the 616 detection units, with a mean value of -1.409% /°C.

Some studies presented their temperature coefficient of the BGO detection units, however, these results are not identical because of the differences of the art of crystal growth and the readout system. We tested the temperature dependence of a 300 mm BGO crystal bar coupled with a PMT, which were used in the DAMPE quarter prototype. The Ct value is -1.82% /°C for this BGO-PMT unit [9]. ATIC also utilized the variation of muon MIPs MPV to measure the Ct value with all contributions of the detector and electronics, whose mean value is -1.86% /°C [15]. Other results about temperature coefficients of the BGO crystal detection units are approximately -1.2% /°C for reference [16, 17].

Since the PMTs, the electronics and the BGO crystals were not calibrated separately, it was hardly to derive the temperature sensitivity for the BGO crystals themselves. To further understand the unit to unit difference of C_t values, we compare the C_t values of both sides of one BGO crystal bar. This eliminates the individual variation of crystals, and the difference of the PMTs and electronics is emerged. Additionally, the uncertainties of the Side 1 C_t values in layer 2 ~ layer 13 should be larger than Side 0 because of more attenuation applied in Side 1, which affected the

2016 JINST 11 T07003

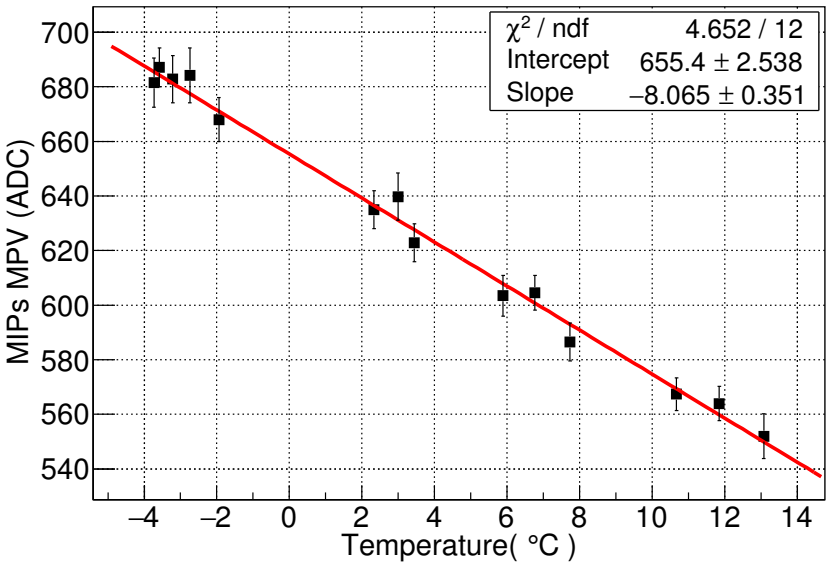

Figure 7. The variation of MIPs MPV values with temperature.

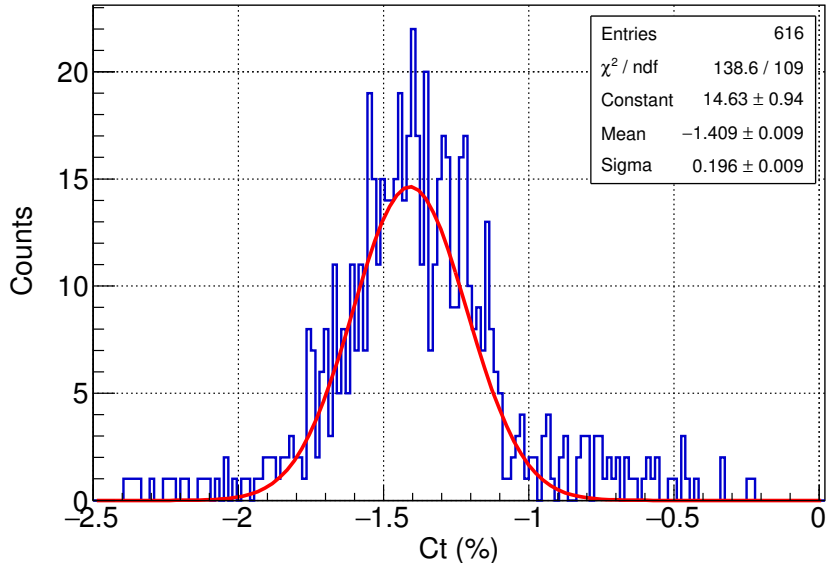

Figure 8. Temperature coefficient distribution of 308 BGO crystal unit.

2016 JINST 11 T07003

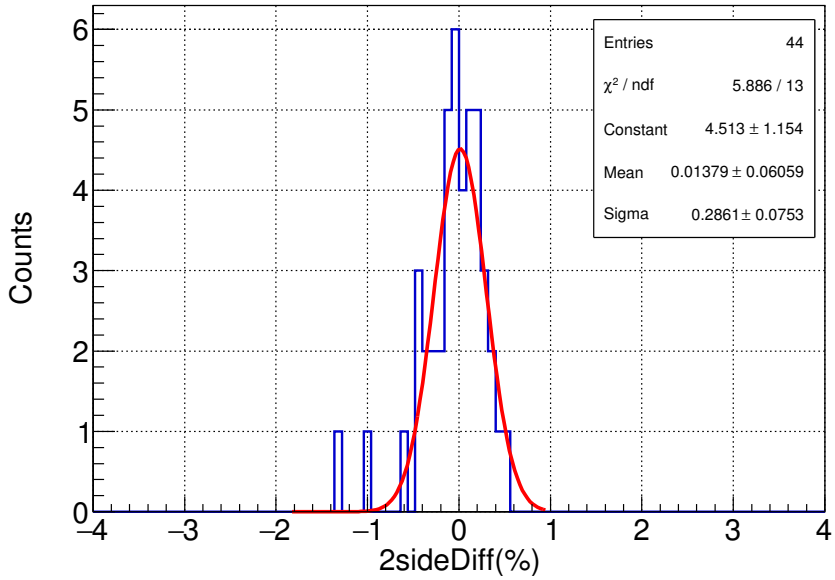

Figure 9. The difference of two sides C_t values.

energy resolution and the accuracy of the MIPs MPV measurement. Thus, to be comparable, a total of 88 detection units in the layer 1 and layer 14, with the same attenuation filters, are chosen in this two side comparison. The difference of two sides of C_t values are shown in figure 9, which indicates that except the crystals, the individual difference of PMT-electronics readout system also significantly contributed to the distribution of the C_t values in figure 8.

4.3 Temperature dependence of the PMT dynode ratios

Besides the MIPs MPV variation, another point should be made clear. Only dynode 8 (high gain) can produce a significant signal when a muon MIP deposits its energy in a BGO crystal bar, while the ADC counts of dynode 2 and 5 are very small. Especially for dynode 2, the signal is not able to be separated from the pedestal noise. The coefficient calibrated with muon MIPs can only represent the temperature dependence of dynode 8. Therefore, the temperature dependence of the dynode ratio of dynode 8 ADC to dynode 5 ADC was investigated. It was calibrated by rare shower events of cosmic ray muons. Figure 10 shows the change of the dynode 8/dynode 5 ratio with time. It is clear that the dynode 8/dynode 5 ratio has no obvious temperature dependence, and the plateau exists just because the high voltage was switched to 1000 V mode during July 7 to July 10. Actually, the dynode ratio reflects the gain of PMT, which is relatively stable when the temperature changes. Thus, the temperature dependence of dynode 8 could also represent for other dynodes.

2016 JINST 11 T07003

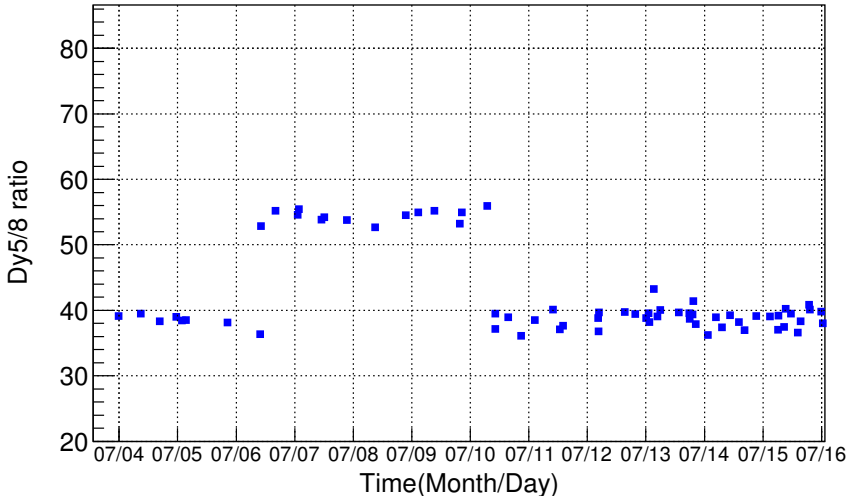

Figure 10. Dynode 8/dynode 5 ratio with time.

5 Temperature effect correction

Based on the results of the temperature dependence calibration, we developed an algorithm for correcting the temperature effect. The correction function is:

$$ADC_{\text{cor}} = \frac{ADC_{\text{raw}}}{C_t \times T + 1} \tag{5.1}$$

where ADC_{raw} is the raw ADC output of the front electronics, ADC_{cor} is the value after temperature correction, T is the temperature of the crystal from which the ADC_{raw} was readout, and C_t is the temperature coefficient. Ignoring the temperature dependence of the dynode ratio, this correction was applied to each output of the three PMT dynodes to compensate for temperature variation event by event, and the ADC counts of all channels were normalized to 0 °C. The cosmic ray from the period of four short thermal cycles (in figure 5) was utilized to validate the temperature correction. Figure 11 shows that the raw MPV values (triangle points) increase synchronously with the temperature decrease, and after correction, the MPV values (circle points) approach to a constant at a reference temperature (0 °C).

To evaluate the correction, the uniformity of MPV value is defined as:

$$\text{Uniformity} = \frac{\text{RMS}_{\text{MPV}}}{\text{Mean}_{\text{MPV}}} \tag{5.2}$$

where RMS and Mean are statistical parameters of MIPs MPV values measured in different temperatures. The MPV uniformities of 616 detection units are shown in figure 12, for Side 0, which are improved from about 9% to approximately 2% after correction. Limited to the poorer resolution, the Side 1 result is relatively worse than the Side 0.

2016 JINST 11 T07003

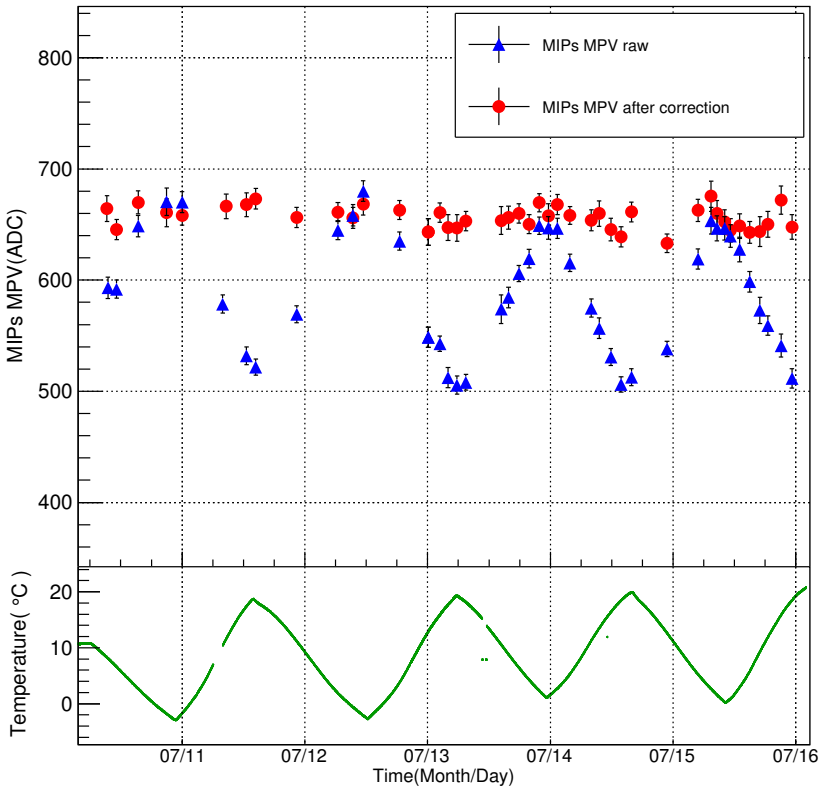

Figure 11. Comparison of muon MIPs MPV value before and after correction.

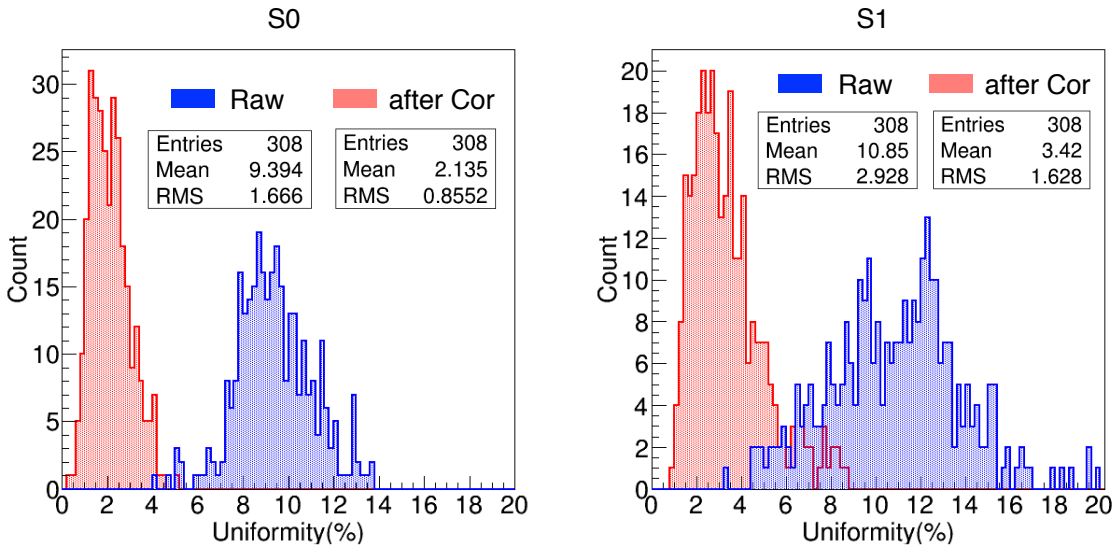

Figure 12. Comparison of MPV uniformity before and after correction.

2016 JINST 11 T07003

6 Conclusion

The temperature performance of the DAMPE flight model BGO calorimeter was studied with a thermal vacuum experiment. The mean value of temperature coefficients for the 616 detection units was measured to be -1.409%. An algorithm was developed to correct the temperature effect, which improves the MPV uniformity significantly. Furthermore, for orbit situation, temperature varies very slow when the satellite does not enter the shadow of the earth. The temperature calibration of the BGO ECAL is still feasible and the calibration parameters will be update in the livetime of the DAMPE.

Acknowledgments

This work was supported by the Chinese 973 Program, Grant No. 2010CB833002, the Strategic Priority Research Program on Space Science of the Chinese Academy of Science, Grant No. XDA04040202-4 and the 100 Talents Program of CAS.

The author would like to thank to the colleagues in the DAMPE collaboration, NUAA (Nanjing University of Aeronautics and Astronautics) and SECM (Shanghai Engineering Center for Microsatellites) for their contributions to the thermal vacuum experiment.

References

[1] AMS collaboration, M. Aguilar et al., *Electron and positron fluxes in primary cosmic rays measured with the Alpha Magnetic Spectrometer on the International Space Station*, *Phys. Rev. Lett.* **113** (2014) 121102.

[2] Fermi-LAT collaboration, A.A. Abdo et al., *Measurement of the cosmic ray e^+ plus e^- spectrum from* 20 *GeV to* 1 *TeV with the Fermi Large Area Telescope*, *Phys. Rev. Lett.* **102** (2009) 181101 [arXiv:0905.0025].

[3] PAMELA collaboration, O. Adriani et al., *The cosmic-ray electron flux measured by the PAMELA experiment between* 1 *and* 625 *GeV*, *Phys. Rev. Lett.* **106** (2011) 201101 [arXiv:1103.2880].

[4] J. Chang, *Dark Matter Particle Explorer: the first Chinese cosmic ray and hard γ-ray detector in space*, *Chinese J. Space Sci.* **34** (2014) 550.

[5] C. Melcher et al., *Temperature dependence of fluorescence decay time and emission spectrum of bismuth germanate*, *IEEE Trans. Nucl. Sci.* **32** (1985) 529.

[6] J. Gironnet, V.B. Mikhailik, H. Kraus, P. de Marcillac and N. Coron, *Scintillation studies of Bi_4-Ge_3-O_{12} (BGO) down to a temperature of* 6*K*, *Nucl. Instrum. Meth.* **A 594** (2008) 358.

[7] Particle Data Group collaboration, K.A. Olive et al., *Review of particle physics*, table 33.4, *Chin. Phys.* **C 38** (2014) 090001.

[8] *Photomultiplier tubes and related products (Hamamatsu)*, page 9, https://www.hamamatsu.com/resources/pdf/etd/PMT_TPMZ0002E.pdf.

[9] P. Wang, Y. Zhang, Z. Xu and X. Wang, *Study on the temperature dependence of BGO light yield*, *Sci. China Phys. Mech. Astron.* **57** (2014) 1898 [arXiv:1309.7646].

[10] Z. Zhang et al., *Design of a high dynamic range photomultiplier base board for the BGO ECAL of DAMPE*, *Nucl. Instrum. Meth.* **A 780** (2015) 21.

2016 JINST 11 T07003

[11] Y.-L. Zhang et al., *A high dynamic range readout unit for a calorimeter*, *Chin. Phys.* **C 36** (2012) 71.

[12] Z. Zhang et al., *The calibration and electron energy reconstruction of the BGO ECAL of the DAMPE detector*, arXiv:1602.07015.

[13] C. Feng et al., *Design of the readout electronics for the BGO calorimeter of DAMPE mission*, *IEEE Trans. Nucl. Sci.* **62** (2015) 3117.

[14] D.-L. Zhang et al., *Onboard calibration circuit for the DAMPE BGO calorimeter front-end electronics*, *Chin. Phys.* **C 40** (2016) 056101 [arXiv:1507.05862].

[15] J. Isbert et al., *Temperature effects in the ATIC BGO calorimeter*, *Adv. Space Res.* **42** (2008) 437.

[16] M. Castoldi et al., *The temperature monitoring system of a BGO calorimeter*, *Nucl. Instrum. Meth.* **A 403** (1998) 22.

[17] A. Zucchiatti, A. Rottura, C. Bernini and G. Gervino, *Temperature behavior of a BGO prototype for use on a* 4π *high-energy spectrometer*, *Nucl. Instrum. Meth.* **A 281** (1989) 341.

2016 JINST 11 T07003